Journal of Organometallic Chemistry 693 (2008) 2541–2550

Contents lists available at ScienceDirect

Journal of Organometallic Chemistry

journal homepage: www.elsevier.com/locate/jorganchem

New di- and triorganotin(IV) derivatives of tyrosinylphenylalanine as models for metal–protein interactions: Synthesis and structural characterization. Crystal structure of Me_2Sn(Tyr-Phe) · MeOH

Mala Nath [a,*], Hitendra Singh [a], George Eng [b], Xueqing Song [b]

[a] Department of Chemistry, Indian Institute of Technology Roorkee, Roorkee 247 667, India
[b] Department of Chemistry and Physics, University of The District of Columbia, Washington, DC 20008, USA

ARTICLE INFO

Article history:
Received 5 March 2008
Received in revised form 17 April 2008
Accepted 23 April 2008
Available online 30 April 2008

Keywords:
Di- and triorganotin(IV) complexes
Tyrosinylphenylalanine
Multinuclear magnetic resonance
^{119}Sn Mössbauer
Crystal structure of Me_2Sn(Tyr-Phe) · MeOH

ABSTRACT

New di- and triorganotin(IV) derivatives of tyrosinylphenylalanine (H_2Tyr-Phe) with general formulae R_2Sn(Tyr-Phe) where R = Me,*n*-Bu, *n*-Oct and Ph, and R'_3Sn(HTyr-Phe) where R′ = Me and Ph have been synthesized. The bonding and coordination behaviour in these derivatives are discussed on the basis of FT-IR, multinuclear ^{1}H, ^{13}C and ^{119}Sn NMR and ^{119}Sn Mössbauer spectroscopic studies. These investigations suggest that dipeptide in R_2Sn(Tyr-Phe) acts as dianionic tridentate coordinating through $-C(O)O^-$, $-NH_2$ and $(-CO)N^-_{peptide}$ groups while in case of R'_3Sn(HTyr-Phe) the ligand acts as monoanionic bidentate coordinating through $-C(O)O^-$ and $-NH_2$, and the polyhedron around tin in R_2Sn(Tyr-Phe) and R'_3Sn(HTyr-Phe) is a distorted trigonal-bipyramidal. It is further confirmed by the single crystal X-ray structure of Me_2Sn(Tyr-Phe) · MeOH which shows two methyl groups and peptide nitrogen ($N^-_{peptide}$) in the equatorial positions, while the two axial positions are occupied by the carboxylic oxygen ($O^-_{carboxyl}$) and the amino nitrogen (N_{amino}) atom from the same ligand molecule. One methanol molecule is also present in the asymmetric unit.

1. Introduction

Metal ions play a very important role in various physico-chemical processes occurring in living organisms and they also emerged as metallopharmaceuticals exhibiting anti-tumour activity. The initial success of platinum chemotherapeutic metallopharmaceuticals attracted a considerable attention of researchers toward non-platinum chemotherapeutics starting from the basic *cis*-platin framework, with the aim to optimize the efficiency of such drugs. Among these, organotins emerged as potential biologically active metallopharmaceuticals in the last thirty years [1,2], although their anti-tumour properties had been reported much earlier [3]. In order to study the behaviour of metallic species inside the biological systems, it is necessary to study their coordination behaviour with ligands that can occur in the biological medium, such as the interaction of organotins with the high-affinity site of ATPase (histidine only) and the low-affinity site of ATPase and haemoglobins (histidine and cystine) [4,5], and hence to formulate structure–activity correlations to explore new compounds with potential anti-tumour activity.

The biological significance of organotin compounds has been established by various studies concentrating on structure–activity correlations [6–13], that dealt mainly with structural aspects and anti-tumour activity. Speciation of organotin compounds in biological systems highlighted two important factors, namely that the $R_nSn^{(4-n)+}$ moiety (where n = 1, 2 and 3) is an active species, which can bind with biological molecules and facilitate the transport to the target site, and that the highest activity may be due to the dissociation of a chelating ligand as a part of the mechanism of inhibition [14]. It has been reported that ligands containing O and N atoms as donor sites are often involved in many organotin compounds with potential anti-tumour activity [15–21].

In view of this, we carried out systematic investigations on the coordination behaviour of organotin(IV) moieties toward biologically relevant ligands like amino acids and peptides [22–34], with the final goal to develop novel biologically active pharmaceuticals. In comparison with diorganotin(IV)–peptide systems [2,9,22,23,28,29,31,35,36], relatively less attention has been paid to the triorganotin(IV)–peptide systems [2,22,27,28,32,34]. The molecular structures of a number of diorganotin(IV) derivatives of dipeptides have also been determined [37–45]. Here we report the synthesis and structural studies of some di- and triorganotin(IV) derivatives of H_2Tyr-Phe and single crystal X-ray structure of Me_2Sn(Tyr-Phe) · MeOH.

* Corresponding author. Tel.: +91 1332 285797; fax: +91 1332 273560.
E-mail address: malanfcy@iitr.ernet.in (M. Nath).

0022-328X/$ - see front matter © 2008 Elsevier B.V. All rights reserved.
doi:10.1016/j.jorganchem.2008.04.032

2. Experimental

2.1. Materials

All of the reactions were carried out under an anhydrous atmosphere. Solvents were dried and distilled before use. Specially dried methanol (99.95% v/v; E. Merck) was dried by refluxing it with Mg metal in presence of iodine as catalyst and then distilled (absolute methanol). Dimethyltin(IV) dichloride, di-*n*-butyltin(IV) oxide, diphenyltin(IV) dichloride, trimethyltin(IV) chloride and triphenyltin(IV) chloride, (E. Merck), di-*n*-octyltin(IV) oxide (Aldrich) and tyrosinylphenylalanine (H_2Tyr-Phe) (Sigma) were used as received.

2.1.1. Synthesis of dimethyltin/diphenyltin(IV) derivatives of H_2Tyr-Phe by sodium chloride method

Tyrosinylphenylalanine (0.656 g; 2.0 mmol) was dissolved in the minimum amount (20 ml) of absolute methanol under dry nitrogen. Sodium methoxide (4.5 equiv.), prepared by dissolving sodium (4.5 equiv.) in absolute methanol (30 ml), was then added. The resulting mixture was first stirred at room temperature for half an hour and then refluxed giving a clear solution of Na_2Tyr-Phe within half an hour. Refluxing was continued for another 4–6 h with constant stirring. A hot methanolic solution (20 ml) of dimethyltin(IV) dichloride (0.44 g, 2.0 mmol)/diphenyltin(IV) dichloride (0.688 g, 2.0 mmol) was added to the solution of the preformed sodium salt (Na_2Tyr-Phe) giving a clear solution. The resulting mixture was further refluxed with constant stirring for another 14–16 h for the diphenyltin(IV) derivative whereas only stirring was carried out at 30 ± 2 °C for the dimethyltin(IV) derivative, under dry nitrogen atmosphere. It was then centrifuged and filtered in order to remove the sodium chloride formed. The excess of solvent was removed under reduced pressure and the solid product thus obtained was recrystallized from either methanol–hexane or methanol–petroleum ether (b.p. 40–60 °C) mixture (1:3 v/v).

Me_2Sn(Tyr-Phe)·MeOH (**1**): Creamish crystalline solid; m.p. 170 °C. Anal. Calc. for $C_{21}H_{28}N_2O_5Sn$: C, 49.73; H, 5.56; N, 5.52; Sn, 23.40. Found: C, 49.55; H, 5.29; N, 5.37; Sn, 23.18%.

Ph_2Sn(Tyr-Phe) (**4**): Creamish white solid; m.p. 130 °C (decomp.). Anal. Calc. for $C_{30}H_{28}N_2O_4Sn$: C, 60.13; H, 4.71; N, 4.67; Sn, 19.81. Found: C, 59.83; H, 4.55; N, 4.43; Sn, 19.35%.

2.1.2. Synthesis of trimethyltin/triphenyltin(IV) derivatives of H_2Tyr-Phe by the sodium chloride method

Tyrosinylphenylalanine (0.656 g; 2.0 mmol) was dissolved in the minimum amount (20 ml) of absolute methanol under dry nitrogen and added to sodium methoxide (2.5 equiv.), prepared by reacting sodium (2.5 equiv.) in absolute methanol (25 ml). The resulting mixture was refluxed with constant stirring giving a clear solution of NaHTyr-Phe within half an hour. Refluxing was continued for another 5–6 h with constant stirring. A hot methanolic solution (20 ml) of trimethyltin(IV) chloride (0.3985 g, 2.0 mmol) or triphenyltin(IV) chloride (0.7710 g, 2.0 mmol) was added to the solution of the preformed sodium salt (NaHTyr-Phe). The resulting solution was further refluxed with constant stirring for another 8–10 h in the case of the triphenyltin(IV) derivative whereas no refluxing was required, only stirring was sufficient for the trimethyltin(IV) derivative. It was then centrifuged and filtered in order to remove the sodium chloride formed. The excess of solvent was removed under reduced pressure. The semi-solid mass obtained was solidified by trituration with petroleum benzene (b.p. 60–80 °C, E. Merck), and recrystallized from methanol–petroleum benzene (b.p. 40–60 °C) mixture (1:3 v/v).

Me_3Sn(HTyr-Phe) (**5**): White solid; m.p. 70–75 °C. Anal. Calc. for $C_{21}H_{28}N_2O_4Sn$: C, 51.35; H, 5.75; N, 5.70; Sn, 24.17. Found: C, 50.96; H, 5.46; N, 5.36; Sn, 23.88%.

Ph_3Sn(HTyr-Phe) (**6**): Yellowish cream solid; m.p. 130–135 °C (decomp.). Anal. Calc. for $C_{36}H_{34}N_2O_4Sn$: C, 63.83; H, 5.06; N, 4.14; Sn, 17.52. Found: C, 63.49; H, 4.51; N, 3.81; Sn, 17.17%.

2.1.3. Synthesis of di-n-butyltin/di-n-octyltin(IV) derivatives of H_2Tyr-Phe by the azeotropic removal of water method

They were prepared under anhydrous nitrogen atmosphere by dropwise addition of a dry, hot methanol solution of di-*n*-butyl- and di-*n*-octyltin(IV) oxide (0.498 g and 0.722 g for 2.0 mmol respectively) to a hot methanol solution of the H_2Tyr-Phe (0.656 g, 2.0 mmol). The mixture obtained was refluxed with constant stirring for at least 14–16 h with azeotropic removal of water. The solution was filtered, and the excess of solvent was removed under reduced pressure and allowed to cool. The solid product thus obtained was recrystallized from either methanol–hexane or methanol–petroleum ether (b.p. 40–60 °C) mixture (1:3 v/v).

n-Bu_2Sn(Tyr-Phe) (**2**): Creamish white solid; m.p. 125–128 °C. Anal. Calc. for $C_{26}H_{36}N_2O_4Sn$: C, 55.84; H, 6.49; N, 5.01; Sn, 21.22. Found: C, 55.39; H, 6.02; N, 4.74; Sn, 20.81%.

n-Oct_2Sn(Tyr-Phe) (**3**): white solid; m.p. 178 °C (decomp.). Anal. Calc. for $C_{34}H_{52}N_2O_4Sn$: C, 60.81; H, 7.80; N, 4.17; Sn, 17.68. Found: C, 60.69; H, 7.54; N, 3.86; Sn, 17.35%.

3. Measurements

The melting points of the synthesized compounds were determined on a Toshniwal capillary melting point apparatus and were uncorrected. Carbon, hydrogen and nitrogen analyses of these compounds were carried out on a VarioEL, CHNS-rapid elemental analyzer. The tin content in the synthesized compounds was determined gravimetrically as SnO_2 [29]. Infrared and far-infrared spectra of the solid compounds were recorded on a Perkin–Elmer 1600 series FT-IR spectrophotometer in the range 4000–400 cm^{-1} from KBr discs and 600–200 cm^{-1} from CsI discs. ^1H and ^{13}C NMR spectra were recorded on a Bruker DRX 300 (300 MHz FT NMR) spectrometer at the Central Drug Research Institute, Lucknow, India, using CD_3OD as solvent and TMS as the internal standard. ^{119}Sn NMR spectra were recorded on a Bruker DRX 500 (500 MHz FT NMR) spectrometer at the Institute Instrumentation Centre, IIT, Roorkee, India, using DMSO-d_6/CD_3OD as solvent and TMS as the internal standard. ^{119}Sn Mössbauer spectra were recorded on Mössbauer spectrometer model MS-900 according to the procedure reported previously [29], at the Department of Chemistry and Physics, University of The District of Columbia, Washington, DC.

Single crystals of Me_2Sn(Tyr-Phe)·MeOH were obtained by recrystallization from methanolic solution after addition of petroleum ether. The X-ray data of Me_2Sn(Tyr-Phe)·MeOH were recorded at 293(2) K with STOE IPDS I diffractometer fitted with graphite monochromated Mo Kα radiation, $\lambda = 0.71073$ Å. The structure was solved by SHELXS-97 and refined by a full matrix least-squares based on F^2 using SHELXL-97 program [46]. The molecular geometry and the cell packing were prepared by PLATON and MERCURY, respectively [47,48] and software used to prepare materials for publication was WINGX publication routines [49]. Atomic parameters and the equivalent values of the anisotropic temperature factors refined for all non-H atoms were included in the model at their calculated positions. The refinement details of all the atoms with relevant details of bond lengths and bond angles have been tabulated in Tables 3–7.

4. Results and discussion

The reactions of R_2SnCl_2 and R_3SnCl (R = Me and Ph) with the sodium salt of H_2Tyr-Phe (formed according to Eq. (1)) in a 1:2 and 1:1 molar ratio, respectively, led to the formation of the complexes according to Eqs. (2) and (3), respectively. Di-*n*-butyltin/di-*n*-octyltin(IV) oxide reacts with H_2Tyr-Phe (as shown in Scheme 1) in equimolar ratio in dry methanol to give the compound under azeotropic removal of water according to Eq. (4).

$$H_2\text{Tyr-Phe} + x\text{NaOMe} \xrightarrow{\text{AbsoluteMeOH}} \text{Na}_2\text{Tyr-Phe/NaHTyr-Phe} + y\text{MeOH} \quad \text{where } x = 1,2;\ y = 2,1 \tag{1}$$

$$R_2SnCl_2 + \text{Na}_2\text{Tyr-Phe} \xrightarrow{\text{AbsoluteMeOH}} R_2\text{Sn(Tyr-Phe)} + 2\text{NaCl} \tag{2}$$

$$R_3SnCl + \text{NaHTyr-Phe} \xrightarrow{\text{AbsoluteMeOH}} R_3\text{Sn(HTyr-Phe)} + \text{NaCl} \tag{3}$$

$$R'_2SnO + H_2\text{Tyr-Phe} \xrightarrow{\text{AbsoluteMeOH}} R'_2\text{Sn(Tyr-Phe)} + H_2O \quad \text{where R = Me and Ph; R}' = n\text{-Bu and } n\text{-Oct} \tag{4}$$

The above reactions were found to be quite feasible and di- and triorganotin(IV) derivatives (except *n*-Oct_2Sn(Tyr-Phe)) were synthesized within ~18–20 h of refluxing. Whereas, the reactions involving the synthesis of *n*-Oct_2Sn(Tyr-Phe) yielded a turbid solution after a prolonged heating, and the solid was obtained from the filtrate after removing the unreacted peptide/di-*n*-octyltin oxide. The resulting derivatives were obtained in good yields (72–81%). All of the derivatives are found to be stable toward air and moisture. Most of the synthesized compounds are soluble in methanol, but sparingly soluble in chloroform and other solvents upon heating. The analytical data of the derivatives, as presented in Section 2.1, suggest that in every instance the resulting compounds crystallized with 1:1 stoichiometry regardless of the proportions of the organotin moiety and dipeptide used.

4.1. Infrared spectral studies

The characteristic IR frequencies (in cm^{-1}) and their assignments for the free H_2Tyr-Phe and its organotin(IV) derivatives are presented in Table 1.

4.1.1. Coordination by amino group

Infrared NH_2 stretching frequencies were used to distinguish coordinated from non-coordinated amino groups of the dipeptide. The position of ν(N–H) bands is influenced by hydrogen bonding, and by coordination of the nitrogen to tin [22]. Very intense absorption bands due to the $\nu(NH_2)$ occurred in the range 3363–2921 cm^{-1} for diorganotin(IV) derivatives and 3430–2960 cm^{-1} for triorganotin(IV) derivatives; which undergoes a substantial lowering when compared to the non-coordinated H_2Tyr-Phe (3466–3274 cm^{-1}). Similar results have been reported for other derivatives, R_2SnL (H_2L = dipeptide) [22,23,28,29,31], R_3SnAA (AA = amino acid) [22,24–26,28,33] and R_3SnHL (H_2L = dipeptide) [22,27,28,32,34], indicating coordination by the amino group to the central tin atom. Further, broadening occurs for all of the derivatives studied, which indicates either overlapping of ν(OH) and ν(NH) vibrations or the presence of inter- and/or intramolecular hydrogen bonding [22,23,27–29,31]. The appearance of a new band of medium intensity in the region ~494–414 cm^{-1} in all of the derivatives studied, which may be assigned to ν(Sn ← N), further confirms the coordination of the amino nitrogen to the organotin(IV) moiety.

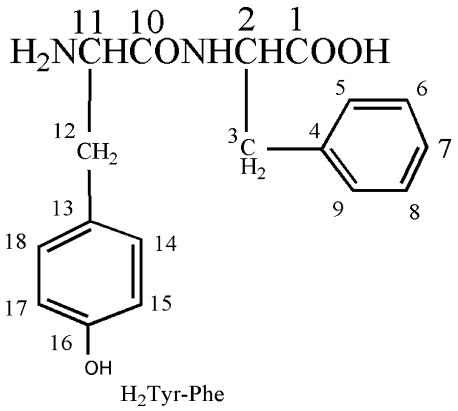

Scheme 1.

4.1.2. Coordination by carboxylate group

The carboxylate groups in the organotin(IV) derivatives generally adopt a bridged structure in the solid state unless the organic substituents at the tin atom are bulky or the carboxylate group is branched at the α-carbon [22]. The IR absorption spectra indicate that $\nu_{as}(C(O)O^-)$ values shown by these amino-coordinated compounds (1613–1584 cm^{-1}) get shifted to higher frequencies in comparison to free H_2Tyr-Phe (1573 cm^{-1}), whereas the corresponding $\nu_s(C(O)O^-)$ absorption frequencies (1404–1361 cm^{-1}) either remain at the same value or move to lower wave number than in the free H_2Tyr-Phe (1404 cm^{-1}). The magnitude of the $(\nu_{as} - \nu_s)C(O)O^-$ ($\Delta\nu$) separation, which has been shown to be useful in identifying structural features, [22] is larger in the amino-coordinated organotin(IV) derivatives ($\Delta\nu$ 234 ± 18 cm^{-1} for Me_2Sn-/*n*-Bu_2Sn(Tyr-Phe) and $\Delta\nu$ 190 ± 6 cm^{-1} for Ph_2Sn-/*n*-Oct_2Sn(Tyr-Phe) and Me_3Sn-/Ph_3Sn(HTyr-Phe)) than in the free H_2Tyr-Phe ($\Delta\nu$ = 169 cm^{-1}) (Table 1). Further, the magnitude of $\Delta\nu$ for all of the derivatives have been found comparable with those obtained for R_2SnL (H_2L = dipeptide), [22,23,28,29,31,35,36] and R_3SnHL (H_2L = dipeptide) [22,27,28,32,34], indicating that the carboxylate group acts as a monodentate ligand, and hence the possibility of ionic bonding and also bridging or chelation can be excluded [22–29,31–34]. Furthermore, the appearance of a new band of medium intensity in the far-IR spectra of all of the derivatives in the region, 566–549 cm^{-1}, which may be assigned to ν(Sn–O), further supports the bonding of $C(O)O^-$ group to the Sn atom [22–29,31–34].

4.1.3. Coordination by peptide group

In the organotin(IV) derivatives studied, apart from the carboxylic oxygen and amino nitrogen as potential coordinating sites to the tin atom, the amide group also exhibits strong tendency to coordinate with the organotin(IV) moiety. Two characteristic bands, *viz*., amide I [essentially ν(C=O)] and amide II [δ(N–H) coupled with ν(C–N)], give the crucial information on the occurrence of metal coordination by the basic atoms of the amide group [50]. The intense band of the amide I observed at 1676 cm^{-1} in H_2Tyr-Phe, undergoes a slight shift to a lower frequency (1640–1613 cm^{-1}) upon coordination in the IR spectra of the diorganotin(IV) derivatives. This is due to the involvement of the peptide nitrogen (because of the deprotonation that has taken place) in bonding with tin, which lowers the bond order of the $(C{=}O)_{amide}$ group due to the resonance stabilization. Further, amide II band observed at 1492 cm^{-1} in H_2Tyr-Phe gets shifted to lower frequency in all of the diorganotin(IV) derivatives with respect to non-coordinated H_2Tyr-Phe, which suggests that the amide nitrogen is the third coordinating site due to the deprotonation of the amide nitrogen.

In trimethyl-/triphenyltin(IV) derivatives studied, an intense band of the amide I (essentially ν(C=O)) at 1676 cm^{-1} in the free H_2Tyr-Phe shifts slightly to 1635 and 1639 cm^{-1}, respectively. The possibility of the involvement of the $(C{=}O)_{amide}$ group in the

Table 1
Characteristic IR frequencies[a] (in cm^{-1}) of di- and triorganotin(IV) derivatives of H_2Tyr-Phe

Complex no.	Ligand/complex	$\nu(NH)_{amino}$/ $\nu(NH)_{pep.}$	$\nu(CO)_{amide}$ ⟨amide I⟩	$\nu_{asym}(OCO)$	$\nu_{sy}(OCO)$	$\Delta\nu$	$\nu_{asy}(Sn–C)$/ $\nu_{sy}(Sn–C)$	ν(Sn–O)	ν(Sn–N)/ ν(Sn ← N)	[δ(NH) + ν(CN)] ⟨amide II⟩
	H_2Tyr-Phe(ligand)	3466 br 3274 br	1676 s	1573 s	1404 m	169				1492 m
1	Me_2Sn(Tyr-Phe). MeOH	3291 s 3208 m 3121 m 3035 w 2939 w	1613 vsbr[b]	1613 vsbr[b]	1396 vs	217	622 m 578 m	557 m	494 m 440 m	Absent
2	*n*-Bu_2Sn(Tyr-Phe)	3261 m 3208 m 3125 m 2957 vs 2926 vs	1625 sh	1613 vsbr[b]	1361 m	252	608 m 571 vw	557 m	490 m 418 vs	Absent
3	*n*-Oct_2Sn(Tyr-Phe)	3363 s 3300 sh 2957 m 2921 vs	1640 s	1584 s	1400 m	184	663 m 602 m	563 s	478 w 414 m	Absent
4	Ph_2Sn(Tyr-Phe)	3345 m 3064 m	1639 s	1590 vs	1396 m	194	280 s 202 s	566 m	456 w 418 w	Absent
5	Me_3Sn(HTyr-Phe)	3408 sbr 2960 s	1635 sh	1596 s	1400 m	196	640 w	549 w	445 w	1506 m
6	Ph_3Sn(HTyr-Phe)	3430 br 3060 w	1639 s	1593 vs	1404 w	189	272 s 210 m	561 w	457 w 445 m	1498 m

[a] Intensity of characteristic bands as vs, very strong; s, strong; m, medium; w, weak; sh, shoulder; br, broad.
[b] Merge with ν(CO) amide.

intermolecular hydrogen bonding cannot be excluded. Further, the amide II band [ν(CN) + δ(NH) as well as ν(NH)], observed at 1492 cm^{-1} in the H_2Tyr-Phe, remains almost unaffected. These observations indicate that the $(C{=}O)_{amide}$ and $(NH)_{peptide}$ groups are not involved in the coordination to the $R_3Sn(IV)$ moiety, instead they may probably be involved in the intermolecular hydrogen bonding, as reported previously for R_3SnHL (H_2L = dipeptide) derivatives [27,28].

The ν_{as}(Sn–C) and ν_s(Sn–C) bands in all of the di- and trialkyltin(IV) derivatives are observed in the range 663–571 cm^{-1}, suggesting the existence of a bent C–Sn–C moiety [22,27–29,31], whereas in the di- and triphenyltin(IV) derivatives, the corresponding ν_{as}(Sn–C) and ν_s(Sn–C) are observed at 276 ± 4 cm^{-1} and 206 ± 4 cm^{-1}, respectively [22,28,29,31,32,34].

4.2. ^{119}Sn Mössbauer spectral studies

The experimental nuclear quadrupole splitting (Q.S.) and isomeric shift (I.S.) values of the solid state R_2Sn(Tyr-Phe) (where R = Me, *n*-Bu, *n*-Oct and Ph), and R'_3Sn(HTyr-Phe) (where R′ = Me and Ph) as presented in Table 2, describe two classes of compounds.

(i) Those having a doublet centered in the region 1.00–1.01 mm s^{-1}; quadrupole splitting (Q.S.) in the region 2.05–2.13 mm s^{-1} for *n*-Oct_2Sn(Tyr-Phe) and Ph_3Sn(HTyr-Phe).

(ii) Those having a doublet centered in the region 1.16–1.26 mm s^{-1}; quadrupole splitting (Q.S.) in the region 2.85–3.04 mm s^{-1} for R_2Sn(Tyr-Phe) (R = Me, *n*-Bu and Ph) and Me_3Sn(HTyr-Phe).

These observations indicate that on going from class (i) to class (ii) compounds, both I.S. and Q.S. values increase due to an increase in s-electron density as well as the large asymmetry of the electron distribution around the tin atom [24,44]. This is probably due to stronger bonding of the dipeptide anion to the dimethyl-/di-*n*-bu-

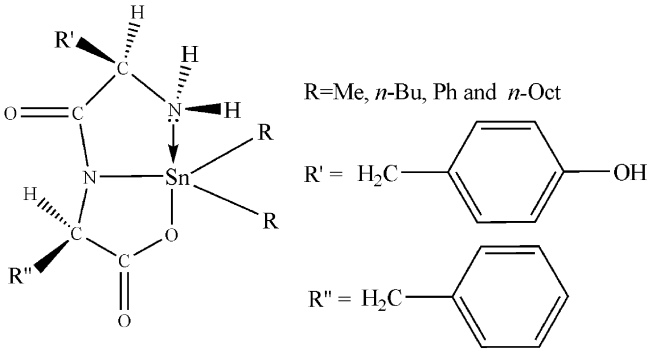

Fig. 1. Structure of diorganotin(IV)tyrosinylphenylalaninates.

Table 2
^{119}Sn Mössbauer data (80 K) of the di- and triorganotin(IV) derivatives of H_2Tyr-Phe

Complex no.[a]	Complex	(Q.S.) (mm s^{-1})	(I.S.) (mm s^{-1})	ρ(Q.S/I.S.)	τ_1(L)	τ_2(R)	∠C–Sn–C[b] (°)
1	Me_2Sn(Tyr-Phe). MeOH	2.85	1.16	2.45	1.28	1.54	123.50
2	*n*-Bu_2Sn(Tyr-Phe)	2.88	1.26	2.28	1.30	1.16	124.34
3	*n*-Oct_2Sn(Tyr-Phe)	2.05	1.01	2.03	1.11	1.15	
4	Ph_2Sn(Tyr-Phe)	2.92	1.20	2.43	1.08	1.03	132.36
5	Me_3Sn(HTyr-Phe)	3.04	1.22	2.49	1.13	1.37	128.80
6	Ph_3Sn(HTyr-Phe)	2.13	1.00	2.13	2.18	2.27	107.01

τ_1(L): half line-width left doublet component; τ_2(R): half line-width right doublet component (mm s^{-1}).
[a] QS: quadrupole splitting; IS: isomeric shift relative to $BaSnO_3$ and tin foil (splitting: 2.52 mm s^{-1}).
[b] Parish relationship Q.S. = $4[R][1 - 3/4\sin^2 2\theta]^{1/2}$; ∠C–Sn–C = 180–2$\theta$° [52].

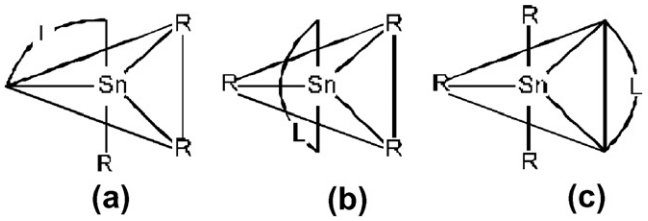

Fig. 2. Structures of three possible isomers of $R_3Sn(HL)$ (where H_2L = a bidentate ligand).

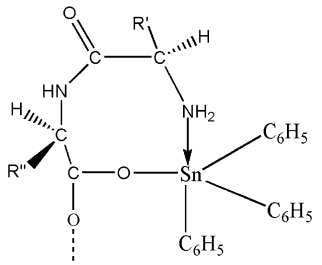

Fig. 4. Proposed structures of triphenyltin(IV) tyrosinylphenylalaninate.

tyl-/diphenyltin(IV) and trimethyltin(IV) moiety than di-*n*-octyl- and triphenyltin(IV) moiety, and partly due to the strain developed in the ligand. It has been reported that the replacement of a smaller alkyl group by a phenyl/octyl group or bulkier group lowers the isomer shift in the organotin(IV) derivatives of the dipeptides/amino acids [22,23,28,33,44,51].

The I.S. and Q.S. values observed in $R_2Sn(IV)$ derivatives of the dipeptides are similar with those of the previously reported complexes [22,28,29,31,44]. The spectroscopic and crystallographic studies reported a distorted trigonal-bipyramidal configuration for $R_2Sn(L)$ (where H_2L = dipeptide), where the organic groups of the organotin(IV) moiety and peptide nitrogen are lying in equatorial position, and the amino nitrogen and carboxylic oxygen atoms are axial [22,28,29,31,37–45]. Due to the high electronegativity of oxygen and nitrogen atom of the dipeptide anion, the Q.S. is mainly governed by ∠C–Sn–C bond angle [52]. The ∠C–Sn–C in the studied

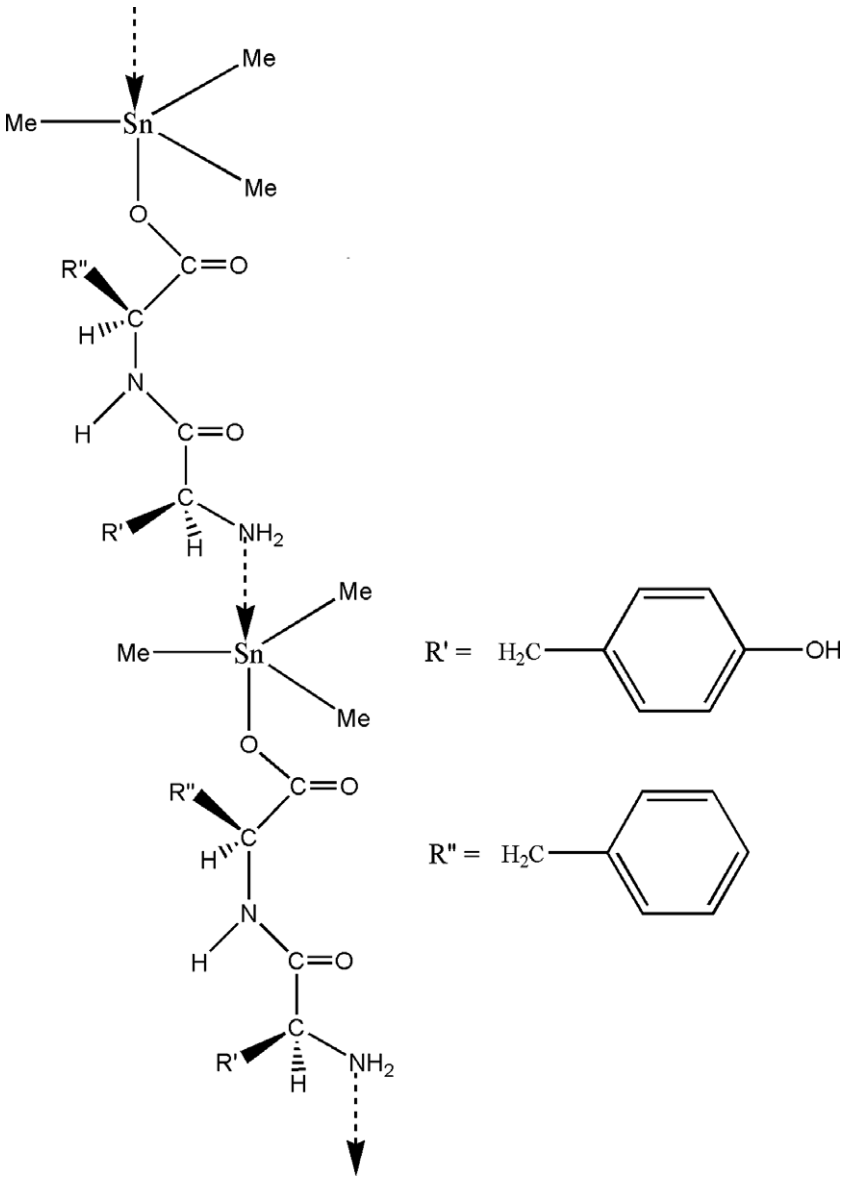

Fig. 3. Proposed structure of trimethyltin(IV) tyrosinylphenylalaninate.

Table 3
Crystal data and structure refinement details of $Me_2Sn(Tyr\text{-}Phe)\cdot MeOH$

Empirical formula	$C_{21}H_{28}N_2O_5Sn$
Formula weight	507.18
Temperature (K)	293(3)
Crystal system	Orthorhombic
Space group	$P2_1$
a (Å)	8.8851(18)
b (Å)	11.173(2)
c (Å)	23.117(5)
α (°)	90
β (°)	90
γ (°)	90
V (Å^3)	2294.8(8)
Z	4
D_{calc} (Mg m^{-3})	1.508
Absorption coefficient (mm^{-1})	1.151
$F(000)$	1056
Crystal size (mm^3)	0.20 × 0.16 × 0.12
θ Ranges for data collection (°)	2.02–26.04
Index ranges	$-10 \leqslant h \leqslant 10$, $-13 \leqslant k \leqslant 13$, $-28 \leqslant l \leqslant 28$
Reflections collected	15792
Independent reflections; R_{int}	4439; 0.1346
Completeness to $\theta = 26.04°$ (%)	98.7
Refinement method	Full-matrix least-squares on F^2
Data/restraints/parameters	4439/0/271
Goodness-of-fit on F^2	1.081
Final R indices [$I > 2\sigma(I)$]	$R_1 = 0.0680$, $wR_2 = 0.1609$
R indices (all data)	$R_1 = 0.0724$, $wR_2 = 0.1660$
Absolute structure parameter	0.01(5)
Largest difference in peak and hole (e Å^{-3})	1.599 and −1.038

diorganotin(IV) derivatives has been calculated by using Parish's relationship [52]: Q.S. = 4[R][1 − (3/4)sin^{2}2θ]$^{1/2}$, where ∠C–Sn–C = (180–2θ)° and [R] is the partial quadruple splitting (p.q.s.) for alkyl and phenyl groups bonded to tin. The reported p.q.s. values of [R] for alkyl and phenyl groups are −1.03 and −0.95 mm s^{-1}, respectively [52,53]. The calculated values of ∠C–Sn–C in the studied diorganotin(IV) derivatives are in the range 123.34–132.36° (Table 2), which are also close to the ∠C–Sn–C observed by the X-ray crystallographic studies of $Me_2Sn(Tyr\text{-}Phe)\cdot MeOH$. Thus, the tin atom configuration as shown in Fig. 1 can be proposed for $R_2Sn(Tyr\text{-}Phe)$, which would then be [tyrosinylphenylalaninato-*O*,*N*,*N*-(2-)diorganotin(IV)], mainly on the basis of the above mentioned similarity between the observed and reported Q.S. values [28,29,31,43], and the calculated ∠C–Sn–C values which are also supported by the X-ray crystallographic data of $Me_2Sn(Tyr\text{-}Phe)\cdot MeOH$.

The Mössbauer spectra of the $R_3Sn(IV)$ (where R = Me, Ph) derivatives exhibit a doublet centered in the I.S. value range 1.00–1.22 mm s^{-1} and the quadrupole splitting (Q.S.) values in the range 2.13–3.04 mm s^{-1}. It has been reported [54,55] that the three conceivable (Fig. 2) five-coordinate isomers of R_3SnL derivatives, where L is a bidentate ligand, have different Q.S. values ranges, 1.7–2.3 mm s^{-1} for isomer (a), 3.0–3.9 mm s^{-1} for (b) and 3.5–4.1 mm s^{-1} for (c).

In $Me_3Sn(HTyr\text{-}Phe)$, the observed values of I.S. and Q.S. lie in the range of *trans*-trigonal-bipyramidal coordination (Fig. 2b) and for $Ph_3Sn(HTyr\text{-}Phe)$, *cis*-trigonal-bipyramidal coordination (Fig. 2a) of tin is found. Therefore, following structures have been proposed for trimethyl-/triphenyltin(IV) derivatives (Figs. 3 and 4), which are also supported by the calculated values of ∠C–Sn–C of 128.80° for trimethyl- and 107.01° for triphenyltin(IV) derivatives (Table 2).

4.3. X-ray crystallographic studies

The crystallographic data and the refinement details are presented in Table 3. Other related data are compiled in Tables 4–7.

The molecular structure of [tyrosinylphenylalaninato-*O*,*N*,*N*-(2-)-dimethyltin(IV)] · methanol (hence forth abbreviated as

Table 4
Selected bond lengths (Å), bond angles (°) and possible hydrogen bonding in $Me_2Sn(Tyr\text{-}Phe)\cdot MeOH$

Bond lengths (Å)					
Sn–C(19)	2.085(8)	N(2)–C(9)	1.336(10)	C(8)–C(9)	1.539(11)
Sn–C(20)	2.100(9)	N(2)–C(10)	1.458(10)	C(10)–C(11)	1.546(12)
Sn–N(2)	2.103(7)	C(1)–C(6)	1.368(13)	C(10)–C(12)	1.551(12)
Sn–O(3)	2.195(5)	C(1)–C(2)	1.403(13)	C(12)–C(13)	1.504(12)
Sn–N(1)	2.251(6)	C(2)–C(3)	1.381(14)	C(13)–C(18)	1.397(13)
O(1)–C(1)	1.369(11)	C(3)–C(4)	1.401(13)	C(13)–C(14)	1.406(14)
O(2)–C(9)	1.238(10)	C(4)–C(5)	1.405(14)	C(14)–C(15)	1.343(15)
O(3)–C(11)	1.269(10)	C(4)–C(7)	1.512(13)	C(15)–C(16)	1.412(18)
O(4)–C(11)	1.251(11)	C(5)–C(6)	1.375(15)	C(16)–C(17)	1.363(18)
N(1)–C(8)	1.489(9)	C(7)–C(8)	1.526(11)	C(17)–C(18)	1.386(16)
				O(1′)–C′	1.346(15)
Bond angles (°)					
C(19)–Sn–C(20)	136.4(4)	C(6)–C(1)–C(2)	119.4(9)	N(2)–C(10)–C(11)	109.1(7)
C(19)–Sn–N(2)	112.4(3)	O(1)–C(1)–C(2)	118.1(9)	N(2)–C(10)–C(12)	113.0(7)
C(20)–Sn–N(2)	110.1(3)	C(3)–C(2)–C(1)	120.6(8)	C(11)–C(10)–C(12)	111.7(7)
C(19)–Sn–O(3)	89.1(3)	C(2)–C(3)–C(4)	120.8(9)	O(4)–C(11)–O(3)	123.6(8)
C(20)–Sn–O(3)	92.5(3)	C(3)–C(4)–C(5)	116.7(10)	O(4)–C(11)–C(10)	118.4(8)
N(2)–Sn–O(3)	75.4(2)	C(3)–C(4)–C(7)	120.8(9)	O(3)–C(11)–C(10)	117.9(7)
C(19)–Sn–N(1)	101.4(3)	C(5)–C(4)–C(7)	122.4(9)	C(13)–C(12)–C(10)	113.7(7)
C(20)–Sn–N(1)	98.8(4)	C(6)–C(5)–C(4)	122.6(9)	C(18)–C(13)–C(14)	117.0(9)
N(2)–Sn–N(1)	74.2(3)	C(1)–C(6)–C(5)	119.8(9)	C(18)–C(13)–C(12)	122.2(8)
O(3)–Sn–N(1)	149.6(3)	C(4)–C(7)–C(8)	116.0(7)	C(14)–C(13)–C(12)	120.8(9)
C(11)–O(3)–Sn	118.0(5)	N(1)–C(8)–C(7)	111.5(6)	C(15)–C(14)–C(13)	122.6(10)
C(8)–N(1)–Sn	109.0(4)	N(1)–C(8)–C(9)	108.5(6)	C(14)–C(15)–C(16)	120.0(11)
C(9)–N(2)–C(10)	120.0(7)	C(7)–C(8)–C(9)	113.5(7)	C(17)–C(16)–C(15)	118.4(11)
C(9)–N(2)–Sn	120.4(6)	O(2)–C(9)–N(2)	126.2(8)	C(16)–C(17)–C(18)	121.8(12)
C(10)–N(2)–Sn	118.6(5)	O(2)–C(9)–C(8)	118.7(7)	C(17)–C(18)–C(13)	120.2(10)
C(6)–C(1)–O(1)	122.5(9)	N(2)–C(9)–C(8)	114.7(7)		

Possible H-bonding (Å, °)				
D–H···A	D–H	D···A	H···A	D–H···A
N(1)–H(1B)···O(3A)	0.86	3.149	2.289	133.5
O(1′)–H(1′A)···O(2)	0.82	2.890	2.070	143.9
O(1)–H(1A)···O(2′)	0.82	2.658	1.838	179.2

Table 5
Atomic coordinates ($\times 10^4$) and equivalent isotropic displacement parameters ($Å^2 \times 10^3$) in Me_2Sn(Tyr-Phe) · MeOH

	x	y	z	U(eq)
Sn	10740(1)	12035(1)	2439(1)	31(1)
O(1)	13294(8)	17066(8)	4614(3)	58(2)
O(2)	14922(7)	11745(5)	3275(3)	44(2)
O(3)	10007(6)	10307(5)	2792(3)	37(1)
O(4)	10408(7)	8907(6)	3457(3)	43(2)
N(1)	12405(7)	13553(6)	2429(4)	43(2)
N(2)	12421(7)	11569(6)	3039(3)	32(2)
C(1)	13711(10)	16310(8)	4177(4)	40(2)
C(2)	13218(10)	16570(8)	3614(4)	43(2)
C(3)	13616(10)	15844(8)	3156(4)	39(2)
C(4)	14518(9)	14831(8)	3242(4)	40(2)
C(5)	14984(11)	14602(9)	3812(5)	49(2)
C(6)	14587(11)	15322(9)	4269(4)	46(2)
C(7)	15014(9)	14069(8)	2736(4)	41(2)
C(8)	13934(8)	13074(7)	2557(4)	36(2)
C(9)	13783(8)	12073(8)	3010(4)	33(2)
C(10)	12168(9)	10543(7)	3416(4)	32(2)
C(11)	10733(10)	9877(8)	3217(4)	36(2)
C(12)	12090(10)	10888(8)	4065(4)	40(2)
C(13)	10929(10)	11829(8)	4198(3)	37(2)
C(14)	11336(12)	13042(10)	4240(4)	49(2)
C(15)	10338(12)	13906(10)	4367(5)	54(3)
C(16)	8811(15)	13613(12)	4459(5)	65(3)
C(17)	8395(13)	12440(12)	4428(6)	67(3)
C(18)	9417(11)	11546(10)	4292(4)	51(2)
C(19)	8888(9)	12842(9)	2831(4)	42(2)
C(20)	11230(12)	11288(8)	1627(4)	43(2)
O(1′)	16403(11)	9685(8)	3628(4)	74(3)
C′	16091(17)	9269(12)	4161(6)	79(4)

U(eq) is defined as one third of the trace of the orthogonalized U^{ij} tensor.

Table 6
Anisotropic displacement parameters ($Å^2 \times 10^3$) in Me_2Sn(Tyr-Phe) · MeOH

	U^{11}	U^{22}	U^{33}	U^{23}	U^{13}	U^{12}
Sn	25(1)	26(1)	41(1)	−1(1)	−2(1)	1(1)
O(1)	47(4)	68(5)	58(4)	−11(4)	−9(3)	10(4)
O(2)	28(3)	34(3)	68(4)	2(3)	−13(3)	5(3)
O(3)	31(3)	23(3)	55(3)	4(3)	−5(3)	−4(2)
O(4)	45(4)	29(3)	56(4)	5(3)	−4(3)	−8(3)
N(1)	22(3)	24(3)	82(6)	1(4)	−10(4)	−2(2)
N(2)	24(3)	27(3)	45(4)	1(3)	−5(3)	1(3)
C(1)	35(4)	38(5)	47(5)	−3(4)	−3(4)	−3(4)
C(2)	35(5)	33(4)	61(6)	8(4)	−4(4)	6(4)
C(3)	35(4)	35(5)	46(5)	8(4)	−6(4)	−6(4)
C(4)	25(4)	35(4)	61(6)	5(4)	−5(4)	−7(3)
C(5)	44(5)	34(5)	68(7)	9(5)	−22(5)	−3(4)
C(6)	45(5)	43(5)	51(5)	6(4)	−14(4)	2(4)
C(7)	17(3)	34(4)	72(6)	−11(4)	0(4)	4(3)
C(8)	22(3)	31(4)	55(5)	−6(4)	9(3)	6(3)
C(9)	26(4)	23(3)	50(4)	1(4)	3(3)	5(3)
C(10)	27(4)	26(4)	43(4)	2(3)	4(4)	5(3)
C(11)	38(4)	30(4)	41(4)	−7(3)	2(4)	−4(4)
C(12)	34(4)	39(5)	47(5)	−1(4)	−10(4)	−1(4)
C(13)	42(5)	34(5)	35(4)	−4(3)	2(4)	−2(4)
C(14)	51(5)	47(6)	50(5)	−5(5)	−7(4)	−3(5)
C(15)	64(7)	42(5)	56(6)	−6(5)	−9(5)	3(5)
C(16)	77(8)	69(8)	48(6)	−4(6)	7(6)	20(7)
C(17)	47(6)	75(8)	80(8)	13(7)	17(6)	8(6)
C(18)	42(5)	53(6)	57(5)	6(5)	8(5)	−8(5)
C(19)	33(4)	34(4)	59(5)	−1(4)	−2(4)	9(4)
C(20)	56(5)	29(4)	44(5)	0(4)	1(4)	11(4)
O(1′)	99(7)	62(5)	62(5)	1(4)	0(5)	40(5)
C′	83(10)	59(8)	95(10)	16(7)	1(8)	9(7)

The anisotropic displacement factor exponent takes the form: $-2\pi^2[h^2a^{*2}U^{11} + \cdots + 2hka^*b^*U^{12}]$.

Me_2Sn(Tyr-Phe) · MeOH) in the asymmetric unit and the numbering of the atoms are shown in Fig. 5 and a stereoscopic view of crystal packing of the unit cell is presented in Fig. 6.

Table 7
Torsion angles (°) in Me_2Sn(Tyr-Phe) · MeOH

C(19)–Sn–O(3)–C(11)	−105.5(6)	C(4)–C(7)–C(8)–C(9)	−67.4(9)
C(20)–Sn–O(3)–C(11)	118.0(6)	C(10)–N(2)–C(9)–O(2)	1.0(13)
N(2)–Sn–O(3)–C(11)	7.9(6)	Sn–N(2)–C(9)–O(2)	−168.0(7)
N(1)–Sn–O(3)–C(11)	5.8(9)	C(10)–N(2)–C(9)–C(8)	174.8(7)
C(19)–Sn–N(1)–C(8)	141.5(6)	Sn–N(2)–C(9)–C(8)	5.8(9)
C(20)–Sn–N(1)–C(8)	−77.4(7)	N(1)–C(8)–C(9)–O(2)	−163.5(8)
N(2)–Sn–N(1)–C(8)	31.1(6)	C(7)–C(8)–C(9)–O(2)	−39.0(10)
O(3)–Sn–N(1)–C(8)	33.3(10)	N(1)–C(8)–C(9)–N(2)	22.2(10)
C(19)–Sn–N(2)–C(9)	−116.9(7)	C(7)–C(8)–C(9)–N(2)	146.7(7)
C(20)–Sn–N(2)–C(9)	72.9(7)	C(9)–N(2)–C(10)–C(11)	−160.5(7)
O(3)–Sn–N(2)–C(9)	160.3(7)	Sn–N(2)–C(10)–C(11)	8.7(8)
N(1)–Sn–N(2)–C(9)	−20.9(6)	C(9)–N(2)–C(10)–C(12)	74.6(9)
C(19)–Sn–N(2)–C(10)	73.9(6)	Sn–N(2)–C(10)–C(12)	−116.2(6)
C(20)–Sn–N(2)–C(10)	−96.2(6)	Sn–O(3)–C(11)–O(4)	179.3(7)
O(3)–Sn–N(2)–C(10)	−8.9(5)	Sn–O(3)–C(11)–C(10)	−5.7(10)
N(1)–Sn–N(2)–C(10)	170.0(6)	N(2)–C(10)–C(11)–O(4)	173.6(7)
C(6)–C(1)–C(2)–C(3)	−0.4(14)	C(12)–C(10)–C(11)–O(4)	−60.8(10)
O(1)–C(1)–C(2)–C(3)	179.4(8)	N(2)–C(10)–C(11)–O(3)	−1.7(10)
C(1)–C(2)–C(3)–C(4)	0.1(14)	C(12)–C(10)–C(11)–O(3)	123.9(8)
C(2)–C(3)–C(4)–C(5)	0.1(13)	N(2)–C(10)–C(12)–C(13)	55.4(10)
C(2)–C(3)–C(4)–C(7)	−177.2(8)	C(11)–C(10)–C(12)–C(13)	−68.1(9)
C(3)–C(4)–C(5)–C(6)	0.1(14)	C(10)–C(12)–C(13)–C(18)	84.3(11)
C(7)–C(4)–C(5)–C(6)	177.3(9)	C(10)–C(12)–C(13)–C(14)	−96.5(10)
O(1)–C(1)–C(6)–C(5)	−179.3(9)	C(18)–C(13)–C(14)–C(15)	0.3(15)
C(2)–C(1)–C(6)–C(5)	0.5(15)	C(12)–C(13)–C(14)–C(15)	−178.9(9)
C(4)–C(5)–C(6)–C(1)	−0.4(15)	C(13)–C(14)–C(15)–C(16)	−0.5(17)
C(3)–C(4)–C(7)–C(8)	−87.4(11)	C(14)–C(15)–C(16)–C(17)	1.4(19)
C(5)–C(4)–C(7)–C(8)	95.5(10)	C(15)–C(16)–C(17)–C(18)	−2(2)
Sn–N(1)–C(8)–C(7)	−162.7(6)	C(16)–C(17)–C(18)–C(13)	1.8(19)
Sn–N(1)–C(8)–C(9)	−37.0(8)	C(14)–C(13)–C(18)–C(17)	−0.8(15)
C(4)–C(7)–C(8)–N(1)	55.4(11)	C(12)–C(13)–C(18)–C(17)	178.4(10)

Symmetry transformations used to generate equivalent atoms.

Me_2Sn(Tyr-Phe) · MeOH crystallizes in the orthorhombic with space group $P2(1)\ 2(1)\ 2(1)$. The asymmetric unit contains one Me_2Sn(Tyr-Phe) molecule and one solvent molecule MeOH. Sn(1) has a considerable distorted trigonal-bipyramidal environment with terminal carboxylate oxygen O(3) (Sn–O(3) = 2.195(5) Å) and terminal amino nitrogen N(1) (Sn–N(1) = 2.251(6) Å) in the axial positions, and deprotonated peptide nitrogen N(2) (Sn–N(2) = 2.103(7) Å) and the two methyl carbons C(19) and C(20) (Sn–C(19) = 2.085(8) Å and Sn–C(20) = 2.100(9) Å) in the equatorial plane into a monomeric unit. The axial angle O(3)–Sn(1)–N(1) of 149.6(3)°, deviates appreciably from linearity. The equatorial angle C(19)–Sn–C(20) in Me_2Sn(Tyr-Phe) · MeOH, 136.4(4)°, is larger than that in pentacoordinated diorganotin(IV)dipeptides (e.g. 117.5(3)° in Ph_2Sn(Gly-Gly) [37]; 123.8(2)° in Me_2Sn(Gly-Met) [39]; 128.7(3)° in Et_2Sn(Gly-His)$_2$ · MeOH [41]; 125.3(3)° in Bu_2Sn(Gly-Val) [44]), but similar to that in Me_2Sn(Met-Met), 132.0(3)° [42]; Me_2Sn(Ala-His), 143.9(2)° [42]; 131.4(2)° in Et_2Sn(Gly-Tyr) [43]. However intermolecular coordination to tin either by carboxylate or peptide oxygen, as the cause of the enlargement of the C–Sn–C angle, can be excluded since Sn–O contacts smaller than 3.5 Å are not experimentally observed [43]. Molecular packing of the compound (Fig. 6) shows three hydrogen bonds: one involving atom N(1) and O(3) with intermolecular N(1)···O(3) distance of 3.149 Å which is almost similar to the sum of the van der Waals radii of 3.11 Å [42]; two hydrogen bonds are present between atoms of adjacent molecules: O(1′) (of tyrosine group)···O(2) (peptide oxygen) and O(1)···O(2′).

4.4. Solution NMR spectral studies

4.4.1. ^{1}H NMR spectral analysis

The characteristic resonance peaks in the ^{1}H NMR spectra of the studied derivatives, recorded in methanol-d_4, are presented in Table 8. The ^{1}H NMR spectral data of H_2Tyr-Phe are also included in Table 8 for comparison. In the ^{1}H NMR spectra of all of the

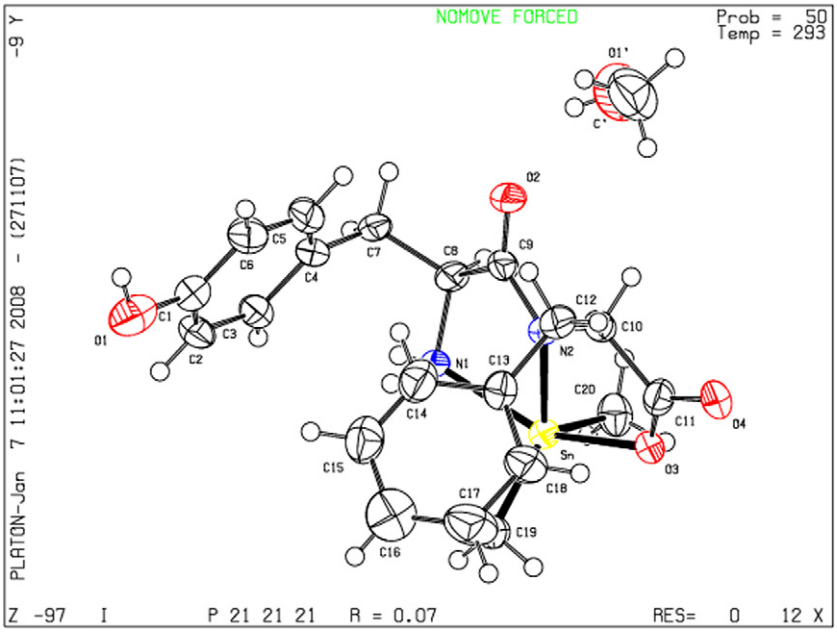

Fig. 5. Molecular structure of $Me_2Sn(Try\text{-}Phe)\cdot MeOH$ view of molecule showing atom numbering scheme.

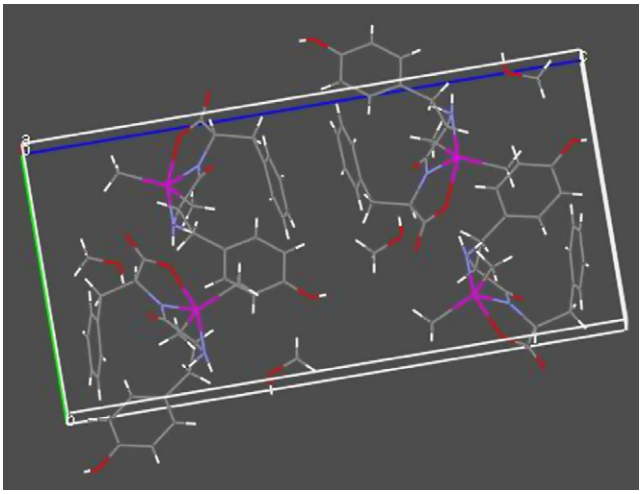

Fig. 6. The molecular packing of $Me_2Sn(Try\text{-}Phe)\cdot MeOH$.

derivatives studied, the -CO(OH) resonance of H_2Tyr-Phe (δ 12.0–13.0 ppm) is absent which suggests the replacement of the carboxylic proton by the organotin(IV) moiety. In all of the diorganotin(IV) derivatives, the -NH_2 resonance observed either as a broad weak signal or in conjugation with phenyl protons attached to the tin, is shifted toward low field in the range δ 7.14–7.84 ppm, when compared to that of H_2Tyr-Phe (δ 5.0–8.0 ppm) [56]. This is probably due to the coordination of the amino group to the organotin(IV) moiety. As reported previously [21–24,26,28,31], upon complexation the magnetically non-equivalent alkyl protons of the ligand undergo the diamagnetic shielding due to the conformation adopted by the ligand molecule. The resonances due to the tin-alkyl protons in the studied Me_2Sn(IV), *n*-Bu_2Sn(IV), *n*-Oct_2Sn(IV) and Me_3Sn(IV) derivatives are observed in the regions δ −0.15–0.58 ppm, δ 0.47–1.53 ppm, δ 0.89–1.50 ppm and δ −0.18–0.39 ppm, respectively, whereas the tin-phenyl protons in the Ph_2Sn(IV) derivative are observed in the regions δ 7.17–7.77 ppm [21–24,26,28,31]. Further the $^2J(^1H–^{119}Sn)$ coupling constant values obtained from the resolved satellites for the Me_2Sn(IV), Me_3Sn(IV) and Ph_2Sn(IV) derivatives correspond to the ∠C–Sn–C of 128.40°, 136.12° and 112.92°/111.45°, respectively, (using Lockhart and Manders equation) [57], which are in close agreement with the crystallographically observed value of ∠C–Sn–C of 136.4° in $Me_2Sn(Tyr\text{-}Phe)\cdot MeOH$ and ∠C–Sn–C values observed from ^{119}Sn Mössbauer data (Table 2) in the solid-state. In the case of *n*-$Bu_2Sn(Tyr\text{-}Phe)$ and *n*-$Oct_2Sn(Tyr\text{-}Phe)$, the satellites are not well resolved hence ^2J values and C–Sn–C angle could not be calculated. In compounds **2**, **3**, **4** and **5**, two set of resonances have been observed due to the presence of stereoisomers. In the case of $Me_3Sn(Tyr\text{-}Phe)$, in addition to the resonance at δ −0.18 ppm [$^2J(^1H–^{119}Sn)$ = 84.0 Hz; ∠C–Sn–C = 136.12], there are two more methyl resonances at δ 0.05 ppm and 0.39 ppm with $^2J(^1H–^{119}Sn)$ values of 54.2 and 63.0 Hz, respectively, which correspond to ∠C–Sn–C of 109.15° and 114.14°, respectively. This indicates that $Me_3Sn(Tyr\text{-}Phe)$ dissociates in the solution to form 4-coordinate Me_4Sn and 5-coordinate $Me_2Sn(Tyr\text{-}Phe)\cdot MeOH$, which are also confirmed by the presence of the corresponding resonances in ^{13}C and ^{119}Sn NMR spectra (discussed in the subsequent sections). The resonances due to all the magnetically non-equivalent protons in the compounds studied have been successfully identified, and the total numbers of protons calculated from the integration curve are in agreement with those calculated from the proposed molecular formula.

4.4.2. ^{13}C NMR spectral analysis

The characteristic resonance peaks in the ^{13}C NMR spectra of all of the studied derivatives, recorded in deuterodimethylsulfoxide/deuteromethanol, are presented in Table 9. The ^{13}C NMR spectral data of H_2Tyr-Phe are also included in Table 9 for comparison. The spectra of the organotin(IV) derivatives of H_2Tyr-Phe are consistent with the following observations:

- The resonances of the carboxylic carbon (i.e., C-1) in compounds **1**, **2**, **3**, **4** and **5** are observed at lower δ (δ 180.6–178.4 ppm) than in H_2Tyr-Phe (δ 208.1 ppm) except in the compound **6** in which the resonance is observed at slightly higher δ (δ 209.2 ppm), suggesting the coordination of H_2Tyr-Phe, through the carboxylic oxygen to the organotin(IV) moiety [22,27–29,31,32].

Table 8
^{1}H NMR spectral data of the di- and triorganotin(IV) derivatives of H_2Tyr-Phe

Complex no.	Complex/ligand (frequency, solvent)	δ[a] (ppm)
Ligand (H_2L)	H_2Tyr-Phe (500 MHz, CD_3OD + DMSO-d_6)	**H-2** + **H-11**: 2.67 (s, 2H); **H-3** + **H-12:** 3.33 (s, 4H); **H-5** + **H-6** + **H-7** + **H-8** + **H-9**: 7.32 (m, 5H); **H-14** + **H-18**: 7.18 (d, 8.0 Hz, 2H); **H-15** + **H-17**: 6.81 (d, 8.0 Hz, 2H)
1	Me_2Sn(Tyr-Phe) · MeOH (300 MHz, CD_3OD)	**H-2**: 4.45 (d, 1.8 Hz, 1H) [31.8 Hz][b]; **H-3**: 3.28, 3.23 (dd, 6.4 Hz, 2H) [14.0 Hz][c]; **H-5** + **H-6** + **H-7** + **H-8** + **H-9**: 7.18 (d, 8.1 Hz, 5H); **H-11**: 3.75, 3.72 (dd, 3.0, 3.0 Hz, 1H); **H-12**: 2.87, 2.82 (dd, 9.0 Hz, 2H) [15.0 Hz][c]; **H-14** + **H-18**: 6.94 (t, 3.3 Hz, 2H); **H-15** + **H-17**: 6.84 (d, 6.0 Hz, 2H); **H-α**: −0.15 [78.0 Hz][b], 0.58 (s, 6H) [78.0 Hz][b], ∠C–Sn–C[b] = 128.40°
2	*n*-Bu_2Sn(Tyr-Phe) (300 MHz, CD_3OD)	**H-2**: 4.53 (s br, 1H); **H-3**: 3.41 (s), 3.38 (d, 4.8 Hz, 2H) [15.3 Hz][c]; **H-5** + **H-6** + **H-7** + **H-8** + **H-9**: 7.26 (d, 8.1 Hz, 5H); **H-11**: 3.80 (d, 3.6 Hz, 1H); **H-12**: 3.32 (s), 3.29 (d, 3.6 Hz, 2H), 3.10, 3.05 (dd, 7.8, 7.8 Hz, 2H)[d] [15.3 Hz][c]; **H-14** + **H-18**: 6.96 (d, 7.8 Hz, 2H); **H-15** + **H-17**: 6.93 (d, 8.1 Hz, 2H); **H-α**: 1.38 (t, 7.1 Hz, 4H); **H-β**: 1.53 (m, 2H), 0.70 (m, 1H), 0.47 (m, 1H)[e]; **H-γ**: 1.19 (m, 4H); **H-δ**: 0.95 (t, 6.9 Hz, 3H), 0.90 (t, 6.6 Hz, 3H)[d]
3	*n*-Oct_2Sn(Tyr-Phe) (300 MHz, CD_3OD)	**H-2**: 4.51 (t, 6.0 Hz, 1H); **H-3**: 3.19, 3.14 (dd, 4.8, 5.0 Hz, 2H), 2.88, 2.84 (dd, 3.6, 3.6 Hz, 2H)[d]; **H-5** + **H-6** + **H-7** + **H-8** + **H-9**: 7.18 (m, 5H); **H-11**: 3.43, 3.40 (dd, 3.9, 3.9 Hz, 1H); **H-12**: 3.03, 2.98 (dd, 7.2, 7.2 Hz, 2H), 2.42, 2.38 (dd, 9.0, 9.3 Hz, 2H)[d]; **H-14** + **H-18:** 6.90 (d, 8.1 Hz, 2H); **H-15** + **H-17:** 6.64 (d, 8.1 Hz, 2H); **H-Octyl**: 1.29 (m, 34H)[e]
4	Ph_2Sn(Tyr-Phe) (300 MHz, CD_3OD)	**H-2**: 4.50 (t, 5.4 Hz, 1H); **H-3**: 3.18, 3.14 (dd, 5.1, 4.8 Hz, 2H), 2.89, 2.84 (dd, 3.9, 3.9 Hz, 2H)[d]; **H-5** + **H-6** + **H-7** + **H-8** + **H-9** + **H -β**: 7.17 (m, 9H); **H-11:** 3.44, 3.41 (dd, 3.9, 4.2 Hz, 1H); **H-12:** 3.03, 2.98 (dd, 7.5, 7.2 Hz, 2H), 2.50, 2.45 (dd, 8.4, 8.7 Hz, 2H)[d]; **H-14** + **H-18:** 6.95 (d, 8.4 Hz, 2H); **H-15** + **H-17**: 6.69 (d, 8.1 Hz, 2H); **H-α**: 7.77 (d, 6.0 Hz, 4H) [61.2/58.8 Hz][b], ∠C–Sn–C[b] = 112.92°/111.45°; **H-γ**: 7.43 (d, 6.9 Hz, 2H)
5	Me_3Sn(HTyr-Phe) (500 MHz, CD_3OD)	**H-2**: 4.91 (s, 1H); **H-3**: 3.18, 3.13 (dd, 6.4 Hz, 2H), 2.85, 2.84 (dd, 6.4 Hz, 2H)[d]; **H-5** + **H-6** + **H-7** + **H-8** + **H-9**: 7.18 (m, 5H); **H-11**: 3.60 (t, 5.5 Hz, 1H); **H-12**: 3.44, 3.41 (dd, 4.2, 3.6 Hz, 2H), 2.44, 2.40 (dd, 6.0 Hz, 2H)[d]; **H-14** + **H-18**: 6.91 (d, 4.2 Hz, 2H); **H-15** + **H-17**: 6.64 (d, 4.0 Hz, 2H); **H-α**: −0.18(s) [84.0 Hz][b], ∠C–Sn–C[b] = 136.12°, 0.05 (s, 9H) [54.2 Hz][b], ∠C–Sn–C[b] = 109.15°, 0.39 (s) [63.0 Hz][b], ∠C–Sn–C[b] = 114.14°

[a] Homonuclear proton–proton coupling multiplet abbreviations given in parentheses: s, singlet; d, doublet; t, triplet; q, quartet; dd, doubledoublet; m, multiplet.
[b] $^2J/^3J(^1H–^{117/119}Sn)$ coupling constants for the alkyl/phenyl groups are given between square brackets and ∠C–Sn–C[b] = $0.0161|^2J| - 1.32|^2J|^2 + 133.4$ [57].
[c] Geminal coupling.
[d] Two set of resonances.
[e] Overlapping multiplets.

Table 9
^{13}C NMR spectral data of the di- and triorganotin(IV) derivatives of H_2Tyr-Phe

Complex no.	Complex/ligand (frequency, solvent)	δ (ppm)
Ligand (H_2L)	H_2Tyr-Phe (500 MHz, CD_3OD + DMSO-d_6)	**C-1**: 208.1; **C-2**: 54.6; **C-3** + **H-12**: 37.8; **C-4**: 132.2; **C-5** + **H-9**: 129.2; **C-6** + **H-8**: 128.1; **C-7**: 126.3; **C-10**: 207.8; **C-11**: 56.0; **C-13**: 139.0; **C-14** + **H-18**: 130.5; **C-15** + **H-17**: 115.6; **C-16**: 156.8
1	Me_2Sn(Tyr-Phe) · MeOH (300 MHz, CD_3OD)	**C-1**: 179.4; **C-2**: 57.4; **C-3**: 37.4; **C-4**: 128.0; **C-5** + **C-6** + **C-8** + **C-9**: 129.3; **C-7**: 127.8; **C-10**: 175.1; **C-11**: 58.6; **C-12**: 39.0; **C-13**: 138.2; **C-14** + **C-18**: **131.7**, **131.5**; **C-15** + **C-17**: **117.0**; **C-16**: 158.3; **C-α**: −0.6, −1.4
2	*n*-Bu_2Sn(Tyr-Phe) (300 MHz, CD_3OD)	**C-1**: 179.4; **C-2**: 57.4; **C-3**: 37.6; **C-4** + **C-7**: 127.8; **C-5** + **C-9**: 131.4; **C-6** + **C-8**: 129.3; **C-10**: 175.1; **C-11**: 58.8; **C-12**: 38.7; **C-13**: 138.1; **C-14** + **C-18**: 131.9; **C-15** + **C-17**: 116.9; **C-16**: 158.0; **C-α**: 20.2, 20.1[a] [610.5 Hz][b], ∠C–Sn–C[b] = 135.78 ± 0.09°; **C-β**: 28.1, 28.2; **C-γ**: 27.5; **C-δ**: 13.9
4	Ph_2Sn (Tyr-Phe) (300 MHz, CD_3OD)	**C-1**: 178.2; **C-2**: 56.8; **C-3**: 39.3; **C-4**: 130.1; **C-5** + **H-9**: 129.2; **C-6** + **H-8**: 129.1; **C-7**: 127.3; **C-10**: 176.1; **C-11**: 57.7; **C-12**: 41.0; **C-13**: 139.3; **C-14** + **H-18**: 131.3; **C-15** + **H-17**: 117.0 (116.7); **C-16:** 158.1; **C-α**: 141.0; **C-β**: 137.6 [37.7 Hz][b]; **C-γ**: 129.7; **C-δ**: 130.5, 130.6
5	Me_3Sn(HTyr-Phe) (500 MHz, CD_3OD)	**C-1**: 180.6, 178.4; **C-2**: 54.9, 55.8; **C-3**: 39.5, 39.2; **C-4**: 127.2; **C-5** + **C-9**: 131.3, 130.8; **C-6** + **C-8:** 129.5, 129.2; **C-7:** 127.4; **C-10**: 176.4, 176.0; **C-11**: (58.7), 58.0, 57.6, 57.0; **C-12**: (42.9), 41.3; **C-13**: 139.5, (138.3), 136.8; **C-14** + **C-18**: 132.2, 131.6; **C-15** + **C-17**: 118.8, 119.5; **C-16**: 161.5; **C-α**: −3.8, −1.2, −0.3
6	Ph_3Sn(HTyr-Phe) (500 MHz, CD_3OD)	**C-1**: 209.2; **C-2** + **C-11**: 54.3; **C-3** + **H-12**: 30.4, 30.3, 30.1; **C-4**: 130.1; **C-5** + **H-9**: 128.6; **C-6** + **H-8**: 130.5, 130.4; **C-7:** 127.0; **C-10**: 176.2; **C-13**: 137.6; **C-14** + **H-18**: 131.6; **C-15** + **H-17**: 119.1; **C-16:** 158.2; **C-α**: 143.0; **C-β**: 137.4; **C-γ**: 129.0; **C-δ**: 129.6

[a] Splitted peak.
[b] $^1J(^{13}C–^{117/119}Sn)$ coupling constants are given between square brackets; weak signals are in parentheses, $|^1J(^{13}C–^{119}Sn)| = (9.99 \pm 0.73)\theta - (746 \pm 100)$ [58].

- Various carbons of H_2Tyr-Phe; especially C-2, undergo a shift to higher δ upon complexation as compared with that of H_2Tyr-Phe, indicating the strong interactions of the O–C═O with tin.
- The carbons of phenyl (δ 129.0–143.0 ppm) and alkyl (δ −3.8 to 28.2 ppm) groups attached to tin are observed at positions comparable with other, similar compounds [22,23,27–29,31,32]. The observed $^1J(^{13}C–^{119}Sn)$ value for *n*-Bu_2Sn(IV) derivative (610.5 Hz) corresponds to ∠C–Sn–C of 135.78 ± 0.09° (using Lockhart and Manders equation) [57,58], which is also in good agreement with the ∠C–Sn–C values obtained for diorganotin(IV) derivatives from ^{119}Sn Mössbauer and X-ray crystallographic data in the solid state. In other derivatives studied herein, the well resolved satellites have not been obtained, hence $^1J(^{13}C–^{119}Sn)$ and ∠C–Sn–C have not been calculated.
- The resonances of the $(CO)_{peptide}$ also get substantial upfield shift (δ 175.1–176.4 ppm) in comparison to that of H_2Tyr-Phe (δ 207.8 ppm) due to the presence of the inter-/intra-molecular hydrogen bonding to the some extent. Moreover, in Me_3Sn(H-Tyr-Phe), two set of resonances have been observed.

4.4.3. ^{119}Sn NMR spectral analysis

The characteristic resonance peaks in the ^{119}Sn NMR spectra of all of the studied derivatives **1**, **2**, **3**, **4**, **5** and **6** recorded in deuteromethanol, are presented in Table 10. The ^{119}Sn chemical shifts of Me_2Sn(Tyr-Phe), *n*-Bu_2Sn(Tyr-Phe), Ph_2Sn(Tyr-Phe), *n*-Oct_2Sn(Tyr-Phe), Me_3Sn(HTyr-Phe), and Ph_3Sn(HTyr-Phe) are observed in the range δ +58.6 to −181.7 ppm which are characteristic of the five-coordinated dialkyl- and diphenyltin(IV) derivatives

Table 10
^{119}Sn NMR spectral data of the di- and triorganotin(IV) derivatives of H_2Tyr-Phe

Complex no.	Complex (500 MHz, CD_3OD)	δ (ppm)
1	Me_2Sn(Tyr-Phe) · MeOH	−160.56
2	Bu_2Sn(Tyr-Phe)	−140.32
3	Oct_2Sn(Tyr-Phe)	−150.6
4	Ph_2Sn (Tyr-Phe)	−106.64
5	Me_3Sn(HTyr-Phe)	−106.3; +58.6; +3.4
6	Ph_3Sn (HTyr-Phe)	−181.7; −288.2

[22,23,27–29,31,32]. Further, ^{119}Sn NMR spectra of Me_3Sn(HTyr-Phe), and Ph_3Sn(HTyr-Phe) gave additional resonances at δ −106.3 and +3.4 ppm and −288.2 ppm, respectively. In case of Ph_3Sn(HTyr-Phe), it may be due to the presence of diastereoisomers. As reported previously, the presence of additional ^{119}Sn NMR resonances in Me_3Sn(HTyr-Phe) can be due to decomposition reaction as shown in Eq. (5), which is favored by the nucleophilic complexation by the methanol molecule from solvent, which weakens one of the Sn–CH_3 bond that becomes prone to methyl group redistribution:

$$2[(CH_3)_3Sn(HTyr\text{-}Phe)] \rightarrow (CH_3)_4Sn + (CH_3)_2Sn(Tyr\text{-}Phe)\cdot MeOH + H_2Tyr\text{-}Phe \quad (5)$$

On the basis of the coordinating pattern of tyrosinylphenylalanine anion toward di- and triorganotin(IV) moieties as evidenced by solution and solid-state spectroscopic studies, these newly synthesized organotin(IV) derivatives may serve as models for metal–protein interactions.

Acknowledgements

M.N. is thankful to the Department of Science and Technology (DST) for the financial support as this work is a part of major research project (Grant No. SP/S1/F-07/2000) sponsored by the DST, New Delhi, India. H.S. is also grateful to DST (India) for the financial support (JRF). Authors are highly thankful to Prof. Bernd Wrackmeyer and Dr. Walfgang Milius, University of Bayreuth, Germany, for recording and providing X-ray data. Financial support for the Mössbauer work from the National Institute of Biomedical Research Support Program (MBRS/SCORE, GM 08005) is gratefully acknowledged.

Appendix A. Supplementary material

CCDC 660030 contains the supplementary crystallography data for **1**. These data can be obtained free of charge from The Cambridge Crystallographic Data Centre via www.ccdc.cam.ac.uk/data_request/cif. Supplementary data associated with this article can be found, in the online version, at doi:10.1016/j.jorganchem.2008.04.032.

References

[1] A.J. Crowe, P.J. Smith, Chem. Ind. (1980) 200.
[2] M.J. Clarke, F. Zhu, D.R. Frasca, Chem. Rev. 99 (1999) 2511.
[3] W.A. Collier, Z. Hyg. Infektionskr. 110 (1929) 236.
[4] M.S. Rose, E.A. Lock, J. Biochem. 120 (1970) 151.
[5] B.G. Farrow, A.P. Dawson, Eur. J. Biochem. 86 (1978) 85.
[6] A.K. Saxena, F. Huber, Coord. Chem. Rev. 95 (1989) 109 and references cited therein.
[7] R. Barbieri, Inorg. Chim. Acta 191 (1992) 253.
[8] S.P. Gupta, Chem. Rev. 94 (6) (1994) 1507.
[9] M. Gielen, Coord. Chem. Rev. 151 (1996) 41.
[10] D. de Vos, R. Willem, M. Gielen, K.E. van Wingerden, K. Nooter, Metal-Based Drugs 5 (1998) 168.
[11] C.E. Holloway, M. Melnik, Main Group Met. Chem. 23 (2000) 1.
[12] C.E. Holloway, M. Melnik, Main Group Met. Chem. 23 (2000) 331.
[13] M. Gielen (Ed.), Tin-Based Antitumor Drugs, NATO ASI Series, H37, Springer-Verlag, Berlin, 1990.
[14] A.J. Crowe, P.J. Smith, C.J. Cardin, H.E. Parge, F.E. Smith, Cancer Lett. 24 (1984) 45.
[15] M. Gielen, A. El Khloufi, M. Biesemans, R. Willem, J. Meunier-Piret, Polyhedron 11 (1992) 1861.
[16] M. Gielen, P. Lelieveld, D. de Vos, H. Pan, R. Willem, M. Biesemans, H.H. Fiebig, Inorg. Chim. Acta 196 (1992) 115.
[17] S. Xueqing, Y. Zhiqiang, X. Qinglan, L. Jinshan, J. Organomet. Chem. 566 (1998) 103.
[18] M. Gielen, M. Biesemans, D. de Vos, R. Willem, J. Inorg. Biochem. 79 (2000) 139.
[19] C. Camacho-Camacho, D. de Vos, B. Mahieu, M. Gielen, M. Kemmer, M. Biesemans, R. Willem, Main Group Met. Chem. 23 (2000) 381.
[20] M. Kemmer, H. Dalil, M. Biesemans, J.C. Martins, B. Mahieu, E. Horn, D. deVos, E.R.T. Tiekink, R. Willem, M. Gielen, J. Organomet. Chem. 608 (2000) 63.
[21] M. Nath, R. Yadav, M. Gielen, H. Dalil, D. de Vos, G. Eng, Appl. Organomet. Chem. 11 (1997) 727.
[22] M. Nath, S. Pokharia, R. Yadav, Coord. Chem. Rev. 215 (2001) 99 and references cited therein.
[23] M. Nath, R. Yadav, G. Eng, T.T. Nguyen, A. Kumar, J. Organomet. Chem. 577 (1999) 1.
[24] M. Nath, R. Yadav, G. Eng, P. Musingarimi, Appl. Organomet. Chem. 13 (1999) 29.
[25] M. Nath, R. Yadav, G. Eng, P. Musingarimi, J. Chem. Res. (S) (1998) 409; M. Nath, R. Yadav, G. Eng, P. Musingarimi, J. Chem. Res. (M) (1998) 1730.
[26] M. Nath, R. Yadav, Bull. Chem. Soc. Jpn. 70 (1997) 1331; M. Nath, R. Yadav, Bull. Chem. Soc. Jpn. 71 (1998) 1355.
[27] M. Nath, S. Pokharia, G. Eng, X. Song, A. Kumar, M. Gielen, R. Willem, M. Biesemans, Appl. Organomet. Chem. 18 (2004) 460.
[28] M. Nath, S. Pokharia, G. Eng, X. Song, A. Kumar, J. Organomet. Chem. 669 (2003) 109.
[29] M. Nath, S. Pokharia, X. Song, G. Eng, M. Gielen, M. Kemmer, M. Biesemans, R. Willem, D. de Vos, App. Organomet. Chem. 17 (2003) 305.
[30] M. Nath, R. Jairath, G. Eng, X. Song, A. Kumar, Inorg. Chem. Commun. 7 (2004) 1161.
[31] M. Nath, S. Pokharia, G. Eng, X. Song, A. Kumar, Synth. React. Inorg. Met. Org. Chem. 34 (2004) 1689.
[32] M. Nath, S. Pokharia, G. Eng, X. Song, A. Kumar, Eur. J. Med. Chem. 40 (2005) 289.
[33] M. Nath, R. Jairath, G. Eng, X. Song, A. Kumar, Spectrochim. Acta, Part A 62 (2005) 1179.
[34] M. Nath, S. Pokharia, G. Eng, X. Song, A. Kumar, Spectrochim. Acta, Part A 63 (2006) 66.
[35] S.E. Castillo-Blum, N. BarbaBehrens, Coord. Chem. Rev. 196 (2000) 3. and references cited therein.
[36] L. Pellerito, L. Nagy, Coord. Chem. Rev. 224 (2002) 111. and references cited therein.
[37] F. Huber, H.J. Haupt, H. Preut, R. Barbieri, M.T. LoGiudice, Z. Anorg. Allg. Chem. 432 (1977) 51.
[38] R. Barbieri, L. Pellerito, F. Huber, Inorg. Chim. Acta 30 (1978) L321.
[39] H. Preut, B. Mundus, F. Huber, R. Barbieri, Acta Crystallogr., Sect. C C42 (1986) 536.
[40] H. Preut, B. Mundus, F. Huber, R. Barbieri, Acta Crystallogr., Sect. C C45 (1989) 728.
[41] H. Preut, M. Vornefeld, F. Huber, Acta. Crystallogr., Sect. C C47 (1991) 264.
[42] G. Stocco, G. Guli, G. Valle, Acta. Crystallogr., Sect. C C48 (1992) 2116.
[43] M. Vornefeld, F. Huber, H. Preut, G. Ruisi, R. Barbieri, Appl. Organomet. Chem. 6 (1992) 75.
[44] B.M. Glowacki, F. Huber, H. Preut, G. Ruisi, R. Barbieri, Appl. Organomet. Chem. 6 (1992) 83.
[45] M.A. Girasolo, L. Pellerito, G.C. Stocco, G. Valle, J. Chem. Soc., Dalton Trans. (1996) 1195.
[46] G.M. Sheldrick, SHELX 97 and SHELXL 97, Program for Crystal Structure and Refinement, University of Göttingen, Germany, 1997.
[47] A.L. Spek, J. Appl. Crystallogr. 36 (2003) 7.
[48] C.F. Macrae, P.R. Edgington, P. McCabe, E. Pidcock, G.P. Shields, R. Taylor, M. Towler, J. van de Streek, J. Appl. Crystallogr. 39 (2006) 453.
[49] L. Farrugia, WINGX Publication Routines, University of Glasgow, 1998.
[50] L.J. Bellamy, Advances in Infrared Group Frequencies, Methuen, London, 1968 p. 178.
[51] L. Pellerito, M.T. LoGiudice, G.C. Stocco, J.D. Donaldson, S.M. Grimes, P.J. Smith, Polyhedron 4 (1985) 747.
[52] R.V. Parish, C.E. Johnson, J. Chem. Soc. (A) (1971) 1906.
[53] T.K. Sham, G.M. Bancroft, Inorg. Chem. 14 (1975) 2281.
[54] L.E. Khoo, J.P. Charland, E.J. Gabe, F.E. Smith, Inorg. Chim. Acta 128 (1987) 139.
[55] G.M. Bancroft, B.W. Davies, N.C. Payne, T.K. Sham, J. Chem. Soc., Dalton Trans. (1975) 973.
[56] W. Kemp, Organic Spectroscopy, 3rd ed., Macmillan, Hampshire, 1991 p. 175 (Chapter 3).
[57] T.P. Lockhart, W.F. Manders, Inorg. Chem. 25 (1986) 892.
[58] J. Holeček, A. Lyčka, Inorg. Chim. Acta 118 (1986) L15.